

## Diffusion-limited aggregation as a deterministic growth process

L. M. Sander, P. Ramanlal, and E. Ben-Jacob

*Physics Department, University of Michigan, Ann Arbor, Michigan 48109*

(Received 27 June 1985)

A set of deterministic continuum equations is proposed to represent diffusion-limited aggregation. A solution using a Green's-function method gives growth very similar to discrete simulations. The growth equations have no external noise. The relationship to viscous fingering and other growth processes is explored.

Irreversible aggregation of particles into clusters has recently attracted a good deal of attention.<sup>1</sup> When clustering is limited by diffusion a fractal object can be produced, as was first pointed out by Witten and Sander.<sup>2,3</sup> The model they introduced, diffusion-limited aggregation (DLA), is very simple: Random walkers accrete on a cluster one at a time by sticking. Despite its simplicity, the model has defied detailed analysis: None of the standard techniques of statistical physics seems applicable and no convincing first-principles derivation of, say, the fractal dimension exists.

In order to make some progress, it is natural to try to replace the discrete DLA model by a continuum theory in order to focus on the long-range scaling properties which are the central feature of fractals. One set of attempts along these lines has been given.<sup>4</sup> In this approach the density of the growing cluster is replaced by a continuous, coarse-grained function, and the equation governing the probability density of the random walkers is replaced by its average. The result of this kind of mean-field treatment is a smooth, spherical object with fractal dimension  $D = d - 1$ , where  $d$  is the dimension of space. This is probably as good a result as should be expected in a mean-field treatment, but it is not DLA.

To go further, it is necessary to attempt to isolate the essential features of the DLA model. Two separate roads seem open: On the one hand, we could attempt to add noise (associated with the random arrival positions of the discrete accreting particles) to the deterministic equations of the mean-field theory. Some numerical work along these lines has been done.<sup>5</sup> However, there are two objections to this sort of approach: (i) As a DLA cluster grows, we might expect that the growth of large features should correspond to adding many particles. Unless subtle correlations are important, it seems that the replacement of the motion of the walkers with its average should be justified. That is, the noise terms should become unimportant. (ii) Experimental evidence has recently appeared to show that DLA-like objects can be grown in Hele-Shaw cells via viscous fingering. The arrangement differs from the classic work of Saffman and Taylor<sup>6</sup> in such a way as to allow repeated splittings of the fingers. This sort of work was first reported by Paterson<sup>7</sup> and later in more detail by Nittmann, Daccord, and Stanley<sup>8</sup> and Ben-Jacob *et al.*<sup>9</sup> In this case the motion of a continuous fluid has no obvious discreteness and no large noise source, suggesting that DLA is not noise driven. In fact, in Ref. 9 it was suggested, on the basis of observation, that a transition of the pattern from orderly to fractal could be seen as a result of the onset and proliferation of tip-splitting instabilities. External noise only need serve to nucleate the growth.

We are thus led, in this work, to investigate analytically the other obvious road: We suggest that DLA is the result of a deterministic process, that it is the chaotic solution to a set of growth equations (without external noise) which are sensitive to initial conditions. We formulate here such a set of equations and solve them numerically.

Our formulation is in terms of the motion of the interface of the aggregate as fed by the incoming random walkers. The incoming walkers have density  $u(\mathbf{x}, t)$ . We concentrate on the interface motion to avoid unphysically long "tails" in the coarse-grained density which probably lead necessarily to mean-field results.<sup>5</sup> In terms of the Saffman-Taylor problem, we follow Paterson<sup>10</sup> in identifying  $u(\mathbf{x}, t)$  with the pressure field of the viscous fluid which is being moved by the less viscous fluid.

In either case, we have, for a two-dimensional system, in dimensionless units, the set of equations previously proposed<sup>8</sup> for the average growth:

$$\nabla^2 u = 0, \quad (1a)$$

$$v_n = -\hat{n} \cdot \nabla u|_s / 4\pi, \quad (1b)$$

$$u(R_0) = 0, \quad (1c)$$

$$u(\mathbf{x}_s) = 1 - \kappa(\mathbf{x}_s), \quad (1d)$$

$$u(x_{\text{int}}) = 1. \quad (1e)$$

The field  $u$  is held constant at 0 at some large distance  $R_0$  from the interface and at 1 in the interior of the region enclosed by the interface;  $\kappa(\mathbf{x}_s)$  represents the curvature of the interface at a point  $\mathbf{x}_s$ , and  $v_n$  its normal velocity. Equation (1b) has the obvious interpretation that the flux of arriving walkers moves the interface. The form of Eq. (1d) is certainly appropriate for the Saffman-Taylor problem, but it is not clearly applicable to DLA. In fact, the boundary condition for DLA simulations involves only a short-distance cutoff corresponding to the particle size  $a$ . As we will see, we can change the form of Eq. (1d) without seeming to change the physics of the solution much. However, we do need some cutoff—otherwise the interface develops unphysical cusps.<sup>11</sup> A solution to Eq. (1) by direct means (say, by relaxation methods) would be difficult. However, it has recently been shown<sup>12</sup> that a more efficient solution can be given by converting to the integro-differential equation:

$$1 + \frac{1}{4\pi} \int d\mathbf{x}'_s \kappa(\mathbf{x}'_s) \frac{\partial}{\partial n'} G(\mathbf{x}_s, \mathbf{x}'_s) = \int d\mathbf{x}'_s G(\mathbf{x}_s, \mathbf{x}'_s) v_n(\mathbf{x}'_s), \quad (2)$$

$$G(\mathbf{x}, \mathbf{y}) = \ln(\mathbf{x}, \mathbf{y})^2 + \ln(R_0^2 \mathbf{y}^2 - \mathbf{x})^2 - \ln(R_0^2 / \mathbf{y}^2). \quad (3)$$

Here  $G(\mathbf{x}, \mathbf{y})$  is the Green's function for the 2D Laplace equation. The integral on the left-hand side of Eq. (2) is the potential due to a dipole layer of strength  $-\kappa/4\pi$ , which ensures a discontinuous jump in the  $u$  field from 1 in the interior to  $1-\kappa(\mathbf{x}_s)$  on the interface. Parametrizing the interface by  $\theta(s)$ , the angle that the normal to the curve at a distance  $s$  along the arc length makes with respect to a fixed direction in space, and  $S_T$ , the total arc length, we have the following equations of motion for  $\theta(s)$  and  $S_T$ :

$$\dot{\theta}(s) = -\partial v_n / \partial s, \quad (4a)$$

$$\dot{S}_T = \int_0^{S_T} ds \kappa(s) v_n(s). \quad (4b)$$

We invert Eq. (2) numerically to obtain  $v_n$  by discretizing and converting to a matrix equation. Then we use Eq. (4) to step the interface forward in time.

Although Eq. (2) is a more efficient way to generate an evolving interface than relaxation schemes, the computation is limited by the magnitude of the arc length  $S_T$ . This becomes evident with a linear stability analysis of a slightly deformed disk. Following Mullins and Sekerka,<sup>13</sup> we set

$$u = R + \delta_m \cos m\theta, \quad (5)$$

where outside the disk,  $u$  is a solution to the Laplace equation

$$u = A \ln(r) + B + C \cos m\theta / r^m. \quad (6)$$

Using the boundary conditions Eqs. (1c) and (1d) together with the interface velocity Eq. (1b) gives, to order  $\delta_m$ ,

$$\frac{(\dot{\delta}_m / \delta_m)}{(\dot{R} / R)} = (m-1) \left[ 1 - m \frac{(m+1) \ln(R_0/R)}{R-1} \right]. \quad (7)$$

The critical radius  $R_C$  below which the structure collapses due to the effect of surface tension is 1 in our units. The smallest unstable structure that one may expect to find in the growing interface is obtained from Eq. (7) for  $m=2$ :

$$R_S = 6 \ln(R_0/R) + 1 \sim 10. \quad (8)$$

This places natural limitations on the number of grid points required when we discretize the arc length: They should be placed no further than  $R_S$  units apart. Since the number of grid points  $L$  is a measure of the size of the matrix to be set up in Eq. (2), one reaches a computational limit for a

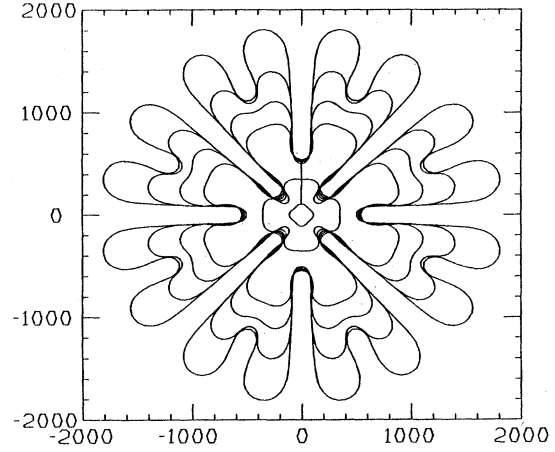


FIG. 1. Growth of a fourfold symmetric structure with  $N=1$ . The  $x$  and  $y$  axes are in units of capillary length.

moderate-sized computer when  $L \sim 4000$  for a fourfold symmetric object. A typical structure at this limit is displayed in Fig. 1, expressing the difficulty of generating a structure anywhere close to physical realizations of multi-branched fluid flow patterns or DLA.

However, suppose we arbitrarily modify Eq. (2):

$$1 + \frac{1}{4\pi} \int dx \kappa^N \frac{\partial G}{\partial n} = \int dx G v_n. \quad (9)$$

The motivation for this replacement is clear for DLA since, in that case, large curvatures  $\kappa > 1/a$  are forbidden, but smaller ones have no effect. For large  $N$  we approach this limit. For fluid flow, however, Eq. (1d) is physically correct.

In order to get some idea of the relationship between solutions for different  $N$  (where  $N$  is an odd integer), we repeat the linear stability analysis to get the following result:

$$\frac{\dot{\delta}_m / \delta_m}{\dot{R} / R} = (m-1) \left[ 1 - \frac{m(m+1) \ln(R_0^N / R^N)}{R^N - 1} \right]. \quad (10)$$

That is, we have effectively rescaled the length in the problem from  $R$  to  $R^N$ . (All lengths are measured in terms of the capillary length for the fluid flow problem, or  $a$  for DLA.)

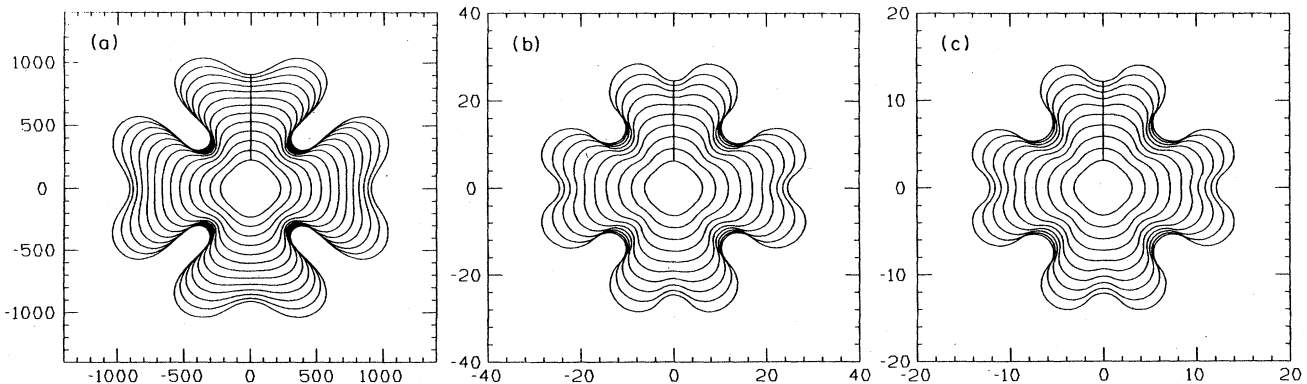


FIG. 2. (a) Growth of a fourfold symmetric structure with  $N=1$  and an initial condition  $R(1 + \delta_m \cos 4\theta)$ .  $R=216$  and  $\delta_m=0.05$ . (b)  $N=3$ , and an initial condition  $R(1 + \delta_m \cos 4\theta)$ .  $R=6$  and  $\delta_m=0.05$ . (c)  $N=5$ , and an initial condition  $R(1 + \delta_m \cos 4\theta)$ .  $R=3$  and  $\delta_m=0.05$ . The  $x$  and  $y$  axes are in units of capillary length.

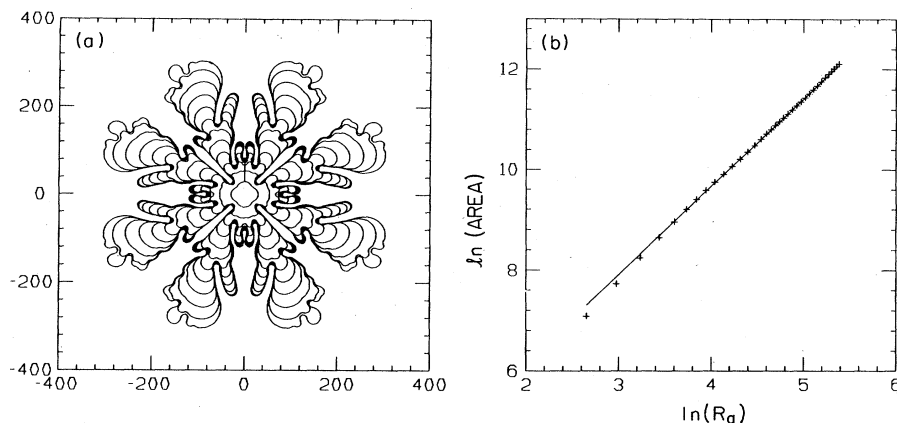


FIG. 3. (a) Growth of a fourfold symmetric structure with  $N=3$ . The  $x$  and  $y$  axes are in units of capillary length. (b) Scaling of area with the radius of gyration.

There are a number of interesting features of Eq. (10). As  $N$  approaches infinity, Eq. (10) approaches the zero surface-tension limit of DLA,<sup>3</sup> and  $R_S$  approaches the lower bound of unity. In fact, as we will see, one approaches the DLA limit for fairly small values of  $N$ . The lower bound of  $R_S$  prevents the formation of cusps and eliminates numerical problems. It also assures the accuracy of the numerical results for grid points no closer than some large fraction of unity, permitting numerical solutions which would otherwise be difficult.

Although the scaling that results from Eq. (10) is based on a linear analysis, it appears to hold approximately even in the nonlinear regime. To show this, we have considered the tip-splitting instability for three appropriately scaled initial conditions  $R(1 + \delta_m \cos m\theta)$  with  $m=4$ ,  $\delta_m=0.05$ , and  $R=216$ , 6, and 3 corresponding to  $N=1$ , 2, and 3. The results are displayed in Fig. 2. Note that the three structures are qualitatively very similar. The computer time required to generate the structures corresponding to  $N=3, 5$  is an order of magnitude less than for  $N=1$ , and up to 2 orders of magnitude for larger structures.

We can now address the question of the kinds of structures that Eq. (1) generates. Values of  $N$  up to 5 are sufficiently large to elucidate the problem. Beginning with a fourfold symmetric initial condition with  $R=20$  and

$\delta_m=0.05$ , we solve Eq. (1), using Eq. (9), for  $N=3, 5$  on a Ridge-32 computer. We obtain the results displayed in Figs. 3(a) and 4(a). The existence of a ramified structure is clear with successive tip splittings, as is the similarity between the numerical results and the patterns observed in a Hele-Shaw cell in experiments of Ben-Jacob *et al.*<sup>9</sup> and Paterson.<sup>7</sup> We think that if we could grow the structure further, we would obtain the wispy structure of DLA. Note, for example, that the thickness of the branches in Figs. 3 and 4 does not seem to increase as fast as the size of the structure. We believe, though we cannot prove, that eventually even for  $N=1$  we will approach the fractal limit.

We can calculate the fractal dimension of the objects in Figs. 3(a) and 4(a) by measuring the scaling of the area with the radius of gyration  $R_g$ :

$$A \sim R_g^D. \quad (11)$$

We find  $D=1.75$  and 1.72 for Figs. 3(b) and 4(b), respectively. The fractal dimension may also be obtained by noting (cf. Ball and Witten)<sup>14</sup>

$$u(r') \sim \ln(r'/R_0)/\ln(R_g/R_0), \quad (12)$$

$$\frac{dN}{dt} \sim R_g^{D-1} \dot{R}_g \sim \int \nabla u \, ds \sim 1/\ln(R_g/R_0).$$

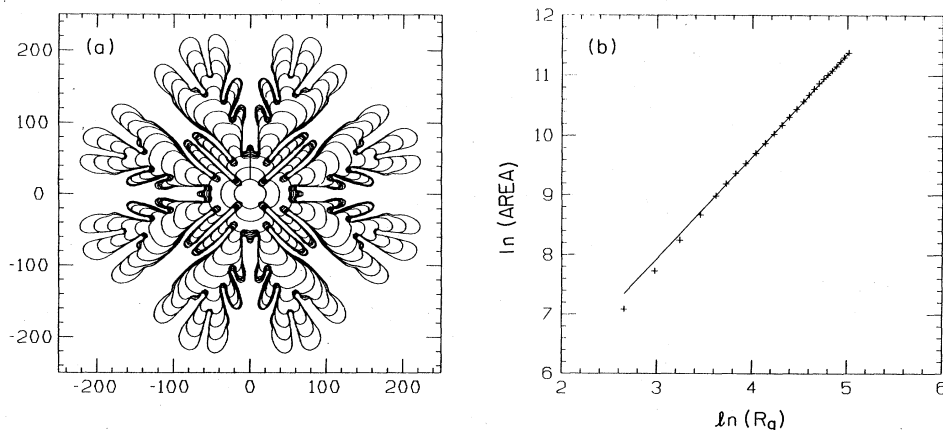


FIG. 4. (a) Growth of a fourfold symmetric structure with  $N=5$ . The  $x$  and  $y$  axes are in units of capillary length. (b) Scaling of area with the radius of gyration.

Upon integrating

$$\frac{t}{\ln(R_0/R_g) + 1/D} \sim R^D, \quad (13)$$

where  $R_0$  is 5000. Equation (13) gives values of  $D$  of 1.75 and 1.76, respectively, in satisfactory agreement with the other estimate.

Finally, we can examine the role of imposed anisotropy. If we model the anisotropy<sup>15</sup> by modifying the boundary condition:

$$u(\mathbf{x}_s) = 1 - \kappa - v_n f(\theta), \quad (14)$$

$$f(\theta) = \beta(1 - \cos m\theta).$$

This modifies Eq. (2):

$$1 + \frac{1}{4\pi} \int dx \kappa \frac{\partial G}{\partial n} = \int dx \left( G - \frac{f(\theta)}{4\pi} \frac{\partial G}{\partial n} \right) v_n. \quad (15)$$

Starting with an initial condition of  $R = 200$ ,  $\delta_m = 0.05$ , and  $m = 4$  with an anisotropic strength  $\beta = 0.004$ , we obtain the structure in Fig. 5. The anisotropy is responsible for the parabolic tip solution and the side branching instability typical of crystalline dendrites in this case, as in the solutions to the boundary-layer<sup>15</sup> and geometrical<sup>16</sup> models, as well as in the experiments of Ben-Jacob *et al.*<sup>9</sup> The tip velocity is observed to oscillate with a periodicity defined by the onset of the side branches, and the tip-splitting instability is suppressed.

In summary, we have tried to show that a model closely related to DLA is sufficiently unstable to give fractal growth, and that the stochasticity of the aggregation process does not seem to play an essential role. The numerical results for the fractal dimension and the general appearance of the structures obtained are reminiscent of computer simulations of DLA and experiments of the viscous finger-

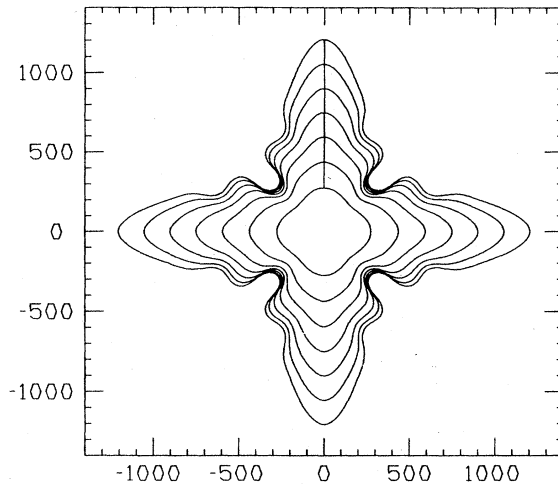


FIG. 5. Growth for  $N=1$  with anisotropy. The  $x$  and  $y$  axes are in units of capillary length.

ing process. We have tried to shed light on the problems with the continuum approximation of DLA; we have also introduced a nontrivial scaling that has made reasonable numerical solutions tractable. Note that even if one declines to accept our risky assumption that the  $N=1$  case is similar to the others, we have demonstrated that for *some* short-range cutoffs we can make DLA-like objects. Finally, we confirm in our nonlocal treatment the role of anisotropy in dendritic solutions, as shown previously in local models<sup>15,16</sup> and for one nonlocal case by Kessler, Koplik, and Levine.<sup>12</sup>

We would like to thank D. Kessler and R. Ball for helpful conversations. This work was supported by U.S. Department of Energy Grant No. DE-FG02-85ER45189.

<sup>1</sup>See *Kinetics of Aggregation and Gelation*, edited by F. Family and D. P. Landau (Elsevier, New York, 1984).

<sup>2</sup>T. A. Witten and L. M. Sander, *Phys. Rev. Lett.* **47**, 1400 (1981).

<sup>3</sup>T. A. Witten and L. M. Sander, *Phys. Rev. B* **27**, 5686 (1983).

<sup>4</sup>R. Ball, M. Nauenberg, and T. A. Witten, *Phys. Rev. A* **29**, 2017 (1984); M. Nauenberg, *Phys. Rev. B* **28**, 449 (1983); M. Nauenberg and L. M. Sander, *Physica A* **123**, 360 (1984).

<sup>5</sup>Y. Kantor and T. A. Witten (unpublished).

<sup>6</sup>P. Saffman and G. Taylor, *Proc. Roy. Soc. London, Ser. A* **245**, 312 (1958).

<sup>7</sup>L. Paterson, *J. Fluid Mech.* **113**, 513 (1981).

<sup>8</sup>J. Nittmann, G. Daccord, and H. E. Stanley, *Nature* **314**, 141 (1985).

<sup>9</sup>E. Ben-Jacob, R. Godbey, N. D. Goldenfeld, J. Koplik, H. Levine, T. Mueller, and L. M. Sander, *Phys. Rev. Lett.* **55**, 1315 (1985).

<sup>10</sup>L. Paterson, *Phys. Rev. Lett.* **52**, 1621 (1984).

<sup>11</sup>B. Shraiman and D. Bensimon, *Phys. Rev. A* **30**, 2840 (1984).

<sup>12</sup>D. A. Kessler, J. Koplik, and H. Levine, *Phys. Rev. A* **30**, 2820 (1984).

<sup>13</sup>W. W. Mullins and R. F. Sekerka, *J. Appl. Phys.* **34**, 323 (1963).

<sup>14</sup>R. Ball and T. A. Witten, *Phys. Rev. A* **29**, 2966 (1984).

<sup>15</sup>E. Ben-Jacob, Nigel Goldenfeld, J. S. Langer, and Gerd Schön, *Phys. Rev. A* **29**, 330 (1984).

<sup>16</sup>R. C. Brower, D. A. Kessler, J. Koplik, and H. Levine, *Phys. Rev. A* **29**, 1335 (1984).